2010 NDIA GROUND VEHICLE SYSTEMS ENGINEERING AND TECHNOLOGY SYMPOSIUM
MODELING & SIMULATION, TESTING AND VALIDATION (MSTV) MINI-SYMPOSIUM
AUGUST 17-19 DEARBORN, MICHIGAN

ADVANCED FUNCTIONALLY GRADED PLATE-TYPE STRUCTURES IMPACTED BY BLAST LOADING

Terry Hause, Ph.D.
Research Mechanical Engineer
U.S. Army RDECOM-TARDEC
Warren, MI 48397

ABSTRACT

The foundation of the theory of functionally graded plates with simply supported edges, under a Friedlander explosive air-blast, are developed within the classical plate theory (CPT). Within the development of the theory, the two constituent phases, ceramic and metal, vary across the wall thickness according to a prescribed power law. The theory includes the geometrical nonlinearities, the dynamic effects, compressive tensile edge loadings, the damping effects, and thermal effects. The static and dynamic solutions are developed leveraging the use of a stress potential with the Extended-Galerkin method and the Runge-Kutta method. Validations with simpler cases within the specialized literature are shown. The analysis focuses on how to alleviate the effects of large deformations through proper material selection and the proper gradation of the constituent phases or materials.

1. INTRODUCTION

During combat situations, the structure of army military vehicles may have to structurally endure the effects of blast loading. Advances in functionally graded materials (FGM's) which combine the properties of two dissimilar materials has been a motivating factor in viewing these types of materials as a viable alternative to the current isotropic metallic structures being utilized in the hull and armor plating. FGM's are microscopically inhomogeneous with thermo-mechanical properties which vary smoothly and continuously from one surface to another. These graded structures allow the integration of dissimilar materials like ceramic and metals that combine different or even incompatible properties such as hardness and toughness.

In this paper, the foundation of the nonlinear theory of functionally graded plate-type structures under an explosive air-blast is developed. An approximate solution methodology for the intricate nonlinear boundary value problem is devised, and results that are likely to contribute to a better understanding of the structural behavior, under an explosive blast with beneficial implications towards their improved design and exploitation are presented.

It is the author's intent, within this paper, to fill in some major gaps currently existing within the specialized literature.

2. BASIC ASSUMPTIONS AND PRELIMINARIES

The plate mid surface is referred to a cartesian orthogonal system of coordinates (x,y,z), while z is the thickness coordinate measured positive in the upwards direction from the mid-surface of the plate with *h* being the uniform plate thickness and *y* is directed perpendicular to the *x*-axis in the plane of the plate. See figure 1 below.

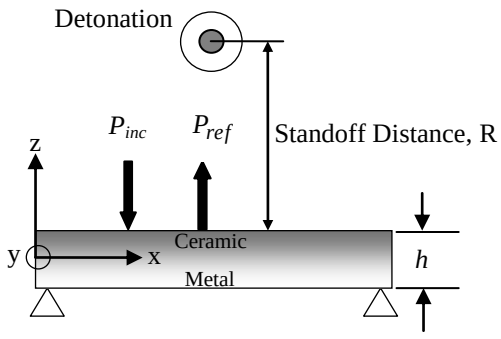

Figure 1: A simply supported functionally graded plate Shown in 2-D, under an explosive blast.

The nonlinear elastic theory of Functionally Graded (FG) Plates is developed using the classical plate deformation Theory [6]. It is also assumed that the FG plate is made-up

of ceramic and metal phases whose material properties vary smoothly and continuously across the wall thickness. By applying the rule of mixtures, the material properties such as Young's Modulus, Density, and Poisson's Ratio are assumed to vary across the wall thickness as

$$P(z) = P_c V_c(z) + P_m V_m(z), \tag{1a}$$

In which P_c and P_m denote the temperature-dependent material properties of the ceramic and metallic phases, of the plate, respectively and may be expressed as a function of temperature [7, 9] as

$$P = P_0 (P_{-1} T^{-1} + 1 + P_1 T + P_2 T^2 + P_3 T^3) \tag{1b}$$

Where, $P_0, P_{-1}, P_1, P_2,$ and P_3 are the coefficients of temperature *T(K)* and are unique to the constituent materials.

$V_c(z)$ and $V_m(z)$ are correspondingly, the volume fractions of the ceramic and metal respectively, fulfilling the relation

$$V_c(z) + V_m(z) = 1. \tag{3}$$

By virtue of (3), Eq. (1a) can be expressed as

$$P(z,T) = [P_c(T) - P_m(T)] V_c(z) + P_m(T). \tag{4}$$

By observation, one can deduce that for $V_c(z) = 0$, $P(z,T) = P_m(T)$ and for $V_c(z) = 1$, $P(z,T) = P_c(T)$. As a result, $V_c(z) \in [0,1]$.

Two Scenarios of the grading of the two basic component phases, ceramic and metal, through the wall thickness are considered.

Case (1): The phases vary symmetrically through the wall thickness, in the sense of having full ceramic at the outer surfaces of the plate and tending toward full metal at the mid-surface. For this case, $V_c(z)$ can be expressed as

$$V_c(z) = \left(\frac{z}{h/2}\right)^N \left(\frac{1+\mathrm{sgn}(z)}{2}\right) + \left(\frac{-z}{h/2}\right)^N \left(\frac{1-\mathrm{sgn}(z)}{2}\right) \tag{5}$$

Where the signum function is defined as

$$\mathrm{sgn}(z) = \begin{cases} 1, & z > 0 \\ 0, & z = 0 \\ -1, & z < 0 \end{cases} \tag{6}$$

N is termed the volume fraction index which provides the material variation profile through the plate wall thickness, $(0 \le N \le \infty)$. A pictorial representation, of the distribution, of the constituent materials are shown below in figure 2.

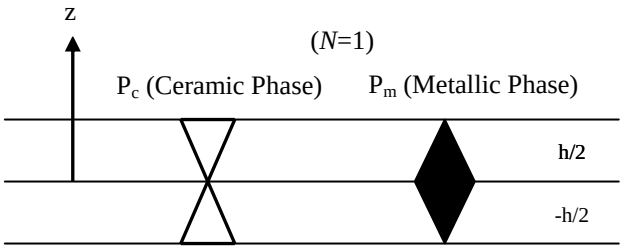

Figure 2: Distribution of the constituent materials through the plate thickness for the symmetric case.

Case (2): The phases vary non-symmetrically through the wall thickness, and in this case there is full ceramic at the outer surface of the plate wall and full metal at its inner surface. For this case, $V_c(z)$ can be expressed as

$$V_c(z) = \left(\frac{h+2z}{2h}\right)^N \tag{7}$$

Below is a pictorial representation of the asymmetric case shown in figure 3.

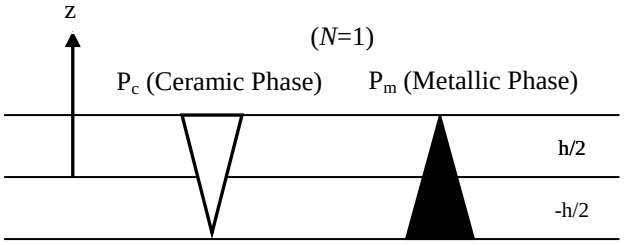

Figure 3: Distribution of the constituent materials through the plate thickness for the asymmetric case.

It should be noted that in contrast to case (2), where there exists coupling between stretching and bending, such coupling is not present for the symmetric case (1). Also, for the purposes of simplicity the Poisson's ratio will be assumed to be constant throughout the plate structure. From equations (1) - (7), the effective material properties of a FG plate can be expressed for the antisymmetric case as

$$\left[E(z,T),\rho(z,T)\right]=\left(E_{cm}(T),\rho_{cm}(T)\right)\left(\frac{h+2z}{2h}\right)^{N}+\left(E_m(T),\rho_m(T)\right) \quad (8)$$

And for the symmetric case as

$$\left[E(z,T),\rho(z,T)\right]=\left(E_{cm}(T),\rho_{cm}(T)\right)\left[\left(\frac{z}{h/2}\right)^{N}\left(\frac{1+\mathrm{sgn}(z)}{2}\right)+\left(\frac{-z}{h/2}\right)^{N}\left(\frac{1-\mathrm{sgn}(z)}{2}\right)\right]+\left(E_m(T),\rho_m(T)\right) \quad (9)$$

$$\nu(z,T)=\nu(T) \quad (10)$$

Where,

$$E_{cm}=E_c-E_m,\ \rho_{cm}=\rho_c-\rho_m \quad (11)$$

3. KINEMATIC EQUATIONS

3.1 The 3-D Displacement Field

Consistent with the classical plate theory [6], the distribution of the 3-D displacement quantities through the wall thickness can be expressed as

$$u(x,y,z,t)=u_0(x,y,t)-z\frac{\partial w_0(x,y,t)}{\partial x},\quad v(x,y,z,t)=v_0(x,y,t)-z\frac{\partial w_0(x,y,t)}{\partial y},\quad w(x,y,z,t)=w_0(x,y,t) \quad (12a\text{-}c)$$

Within these equations, (u,v,w) are the 3-D displacement quantities along the (x,y,z) directions, respectively. While, $u_0, v_0,$ and w_0 are the 2-D displacement quantities of the points on the mid-surface.

3.2 Non-Linear Strain-Displacement Relationships

The nonlinear strain displacement relationships across the plate thickness at a distance from the mid-surface take the form [2, 3, 6]

$$\varepsilon_{xx}=\frac{\partial u}{\partial x}+\frac{1}{2}\left(\frac{\partial w}{\partial x}\right)^2,\ \varepsilon_{yy}=\frac{\partial v}{\partial y}+\frac{1}{2}\left(\frac{\partial w}{\partial y}\right)^2,$$

$$2\varepsilon_{xy}=\gamma_{xy}=\frac{\partial u}{\partial y}+\frac{\partial v}{\partial x}+\frac{\partial w}{\partial x}\frac{\partial w}{\partial y},\ \varepsilon_{xz}=\varepsilon_{yz}=0 \quad (13)$$

Substitution of Equations (12a-c) into Equations (13) results in the strain measures across the plate thickness in terms of the 2-D displacement quantities of the mid-surface of the plate expressed as

$$\begin{Bmatrix}\varepsilon_{xx}\\ \varepsilon_{yy}\\ \gamma_{xy}\end{Bmatrix}=\begin{Bmatrix}\varepsilon_{xx}^{(0)}\\ \varepsilon_{yy}^{(0)}\\ \gamma_{xy}^{(0)}\end{Bmatrix}+z\begin{Bmatrix}\varepsilon_{xx}^{(1)}\\ \varepsilon_{yy}^{(1)}\\ \gamma_{xy}^{(1)}\end{Bmatrix} \quad (14)$$

Where,

$$\left\{\varepsilon^{(0)}\right\}=\begin{Bmatrix}\varepsilon_{xx}^{(0)}\\ \varepsilon_{yy}^{(0)}\\ \gamma_{xy}^{(0)}\end{Bmatrix}=\begin{Bmatrix}\frac{\partial u_0}{\partial x}+\frac{1}{2}\left(\frac{\partial w_0}{\partial x}\right)^2\\ \frac{\partial v_0}{\partial x}+\frac{1}{2}\left(\frac{\partial w_0}{\partial y}\right)^2\\ \frac{\partial u_0}{\partial y}+\frac{\partial v_0}{\partial x}+\frac{\partial w_0}{\partial x}\frac{\partial w_0}{\partial y}\end{Bmatrix},$$

$$\left\{\varepsilon^{(1)}\right\}=\begin{Bmatrix}\varepsilon_{xx}^{(1)}\\ \varepsilon_{yy}^{(1)}\\ \gamma_{xy}^{(1)}\end{Bmatrix}=\begin{Bmatrix}-\frac{\partial^2 w_0}{\partial x^2}\\ -\frac{\partial^2 w_0}{\partial y^2}\\ -2\frac{\partial^2 w_0}{\partial x\partial y}\end{Bmatrix}$$

In the above expressions, $\left(\varepsilon_{xx}^0,\varepsilon_{yy}^0,\gamma_{xy}^0\right)$, are referred to as the membrane strains and $\left(\varepsilon_{xx}^1,\varepsilon_{yy}^1,\gamma_{xy}^1\right)$ are referred to as the flexural bending strains which are also known as the curvatures.

4. CONSTITUTIVE EQUATIONS

The stress-strain relationships for a state of plane stress is expressed as [10]

$$\begin{Bmatrix}\sigma_{xx}\\ \sigma_{yy}\\ \sigma_{xy}\end{Bmatrix}=\begin{bmatrix}Q_{11}&Q_{12}&0\\ Q_{12}&Q_{22}&0\\ 0&0&Q_{66}\end{bmatrix}\begin{Bmatrix}\varepsilon_{xx}-\alpha(z,T)\Delta T\\ \varepsilon_{yy}-\alpha(z,T)\Delta T\\ \gamma_{xy}\end{Bmatrix}$$

$$\sigma_{xz}=\sigma_{yz}=\sigma_{zz}=0 \quad (15)$$

The material stiffnesses, $Q_{ij}(z), (i = 1,2,6)$ are given by [9, 10]

$$Q_{11} = Q_{22} = \frac{E(z,T)}{1-\nu^2},\ Q_{12} = \frac{\nu E(z,T)}{1-\nu^2},$$
$$Q_{66}(z) = \frac{E(z,T)}{2(1+\nu)}, (Q_{16}, Q_{26}) = 0 \qquad (16)$$

The standard force and moment resultants of a plate are defined as

$$\left(N_{ij}, M_{ij}\right) = \int_{-h/2}^{h/2} \sigma_{ij}(1, z)dz, \quad (i, j = x, y, xy) \qquad (17)$$

With the use of Equations (13) –(17), the stress resultants and stress couples are related to the strains by [3]

$$\begin{Bmatrix} N - N^T \\ M - M^T \end{Bmatrix} = \begin{bmatrix} [A] & [B] \\ [B] & [D] \end{bmatrix} \begin{Bmatrix} \varepsilon^{(0)} \\ \varepsilon^{(1)} \end{Bmatrix}, \qquad (18)$$

In which $[A], [B]$, and $[D]$ are the respective in-surface, bending-stretching coupling, and bending stiffnesses. For the case of symmetric FG Plates, $[B] = 0$, since there is no bending-stretching coupling. The global stiffness quantities, A_{ij}, B_{ij}, and D_{ij}, (i, j=1,2,6) are defined as

$$\left(A_{ij}, B_{ij}, D_{ij}\right) = \int_{-h/2}^{h/2} Q_{ij}\left(1, z, z^2\right)dz, \quad (i, j = 1,2,6) \qquad (19)$$

In view of Equations (8), (9), (10), (16), and (19), the global stiffness quantities are determined as

$$\left[(A_{11}, A_{22}), (B_{11}, B_{22}), (D_{11}, D_{22})\right] = \frac{1}{1-\nu^2}(E_1, E_2, E_3),$$
$$(A_{12}, B_{12}, D_{12}) = \frac{\nu}{1-\nu^2}(E_1, E_2, E_3),$$
$$(A_{66}, B_{66}, D_{66}) = \frac{1}{2(1+\nu)}(E_1, E_2, E_3) \qquad (20a\text{-}c)$$

where for the asymmetric case,

$$E_1 = \frac{E_{cm}h}{N+1} + E_{cm}h,\ E_2 = \frac{E_{cm}h^2}{N+2} - \frac{E_{cm}h^2}{2N+2},$$

$$E_3 = E_{cm}h^3\left(\frac{1}{N+3} - \frac{1}{N+2} + \frac{1}{4N+4}\right) + \frac{E_m h^3}{12} \qquad (21)$$

And for the symmetric case,

$$E_1 = \frac{E_{cm}h}{N+1} + E_{cm}h,\ E_2 = 0,\ E_3 = \frac{E_{cm}h^3}{4(N+3)} + \frac{E_m h^3}{12} \qquad (22)$$

5. GOVERNING EQUATIONS

Hamilton's principle is used to derive the equations of motion and the boundary conditions. It is formulated as

$$\delta J = \delta \int_{t_0}^{t_1} (U + V - K)dt = 0, \qquad (23)$$

Where t_0 and t_1 are two arbitrary instants of time. U denotes the strain energy, V denotes the work done by surface tractions, edge loads, and body forces, and K denotes the kinetic energy of the 3-D body of the structure, while δ is the variational operator. In Equation (23), the strain energy is given by

$$\delta U = \int_{\Omega_0} \left[\int_{-\frac{h}{2}}^{\frac{h}{2}} \left(\sigma_{xx}\delta\varepsilon_{xx} + \sigma_{yy}\delta\varepsilon_{yy} + \sigma_{xy}\delta\gamma_{xy}\right)dz \right] d\Omega_0 \qquad (24)$$

where Ω_0 denotes the mid-surface area of the panel. The work done by external loads is expressed as

$$\delta V = -\int_{\Omega_0} \left[P_t(x, y)\delta w\left(x, y, \frac{h}{2}\right) - P_b(x, y)\delta w\left(x, y, -\frac{h}{2}\right) \right] d\Omega_0$$
$$- \int_x \int_{-\frac{h}{2}}^{\frac{h}{2}} \left(\sigma^*_{yy}\delta v + \sigma^*_{yx}\delta u\right)dzdx - \int_y \int_{-\frac{h}{2}}^{\frac{h}{2}} \left(\sigma^*_{xx}\delta u + \sigma^*_{xy}\delta v\right)dzdy \qquad (25)$$

In the above expression, $P_t(x, y)$ is the distributed force at the top surface ($z = h/2$), $P_b(x, y)$ is the distributed force at the bottom surface ($z = -h/2$), $\left(\sigma^*_{xx}, \sigma^*_{yy}, \sigma^*_{xy}, \sigma^*_{yx}\right)$ are the specified stress components along the plate edges, and $(\delta u, \delta v)$ are the virtual displacements along the normal and tangential directions, respectively, along the plate edges. Considering only the transversal inertia of the structure, the kinetic energy is given by

$$K = \frac{1}{2}\int_V \rho_0(z)\dot{W}^2 dV, \tag{26}$$

Which implies that the variation in kinetic energy is expressed as

$$\delta K = \int_{\Omega_0}\int_{-\frac{h}{2}}^{\frac{h}{2}} \rho(z)\dot{W}\delta\dot{W}dzd\Omega_0 \tag{27}$$

where $\rho(z)$ is the mass per unit volume.

Considering Equation (23) in conjunction with Equations (24)-(27) , along with the constitutive equations (15), the strain-displacement relationships, equations (14), and carrying out the integration through the thickness, integrating by parts whenever feasible, using the expression of global stress resultants and stress couples, while retaining only the transversal load, transverse inertia, and transverse damping results in

$$\begin{aligned}
&\int_0^t \left\langle \int_{\Omega_0} \left\{ \left(-\frac{\partial N_{xx}}{\partial x} - \frac{\partial N_{xy}}{\partial y} \right)\delta u_0 + \left(-\frac{\partial N_{yy}}{\partial y} - \frac{\partial N_{xy}}{\partial x} \right)\delta v_0 + \right. \right. \\
&\left[\frac{\partial^2 M_{xx}}{\partial x^2} + 2\frac{\partial^2 M_{xy}}{\partial x \partial y} + \frac{\partial^2 M_{yy}}{\partial y^2} - \frac{\partial}{\partial x}\left(N_{xx}\frac{\partial w_0}{\partial x} + N_{xy}\frac{\partial w_0}{\partial y} \right) \right. \\
&\left. \left. - \frac{\partial}{\partial y}\left(N_{yy}\frac{\partial w_0}{\partial y} + N_{xy}\frac{\partial w_0}{\partial x} \right) + I_0\ddot{w}_0 - P_t(t) - C\dot{w}_0 \right]\delta w_0 \right\} d\Omega_0 \\
&+ \int_y \left\{ \left(N_{xx} - N_{xx}^* \right)\delta u_0 + \left(N_{xy} - N_{xy}^* \right)\delta v_0 - \left(M_{xx} - M_{xx}^* \right)\delta\left(\frac{\partial w_0}{\partial x} \right) \right. \\
&\left. + \left(v_{xx} - v_{xx}^* \right)\delta w_0 \right\}_x dy + \int_x \left\{ \left(N_{yx} - N_{yx}^* \right)\delta u_0 + \left(N_{yy} - N_{yy}^* \right)\delta v_0 - \right. \\
&\left. \left(M_{yy} - M_{yy}^* \right)\delta\left(\frac{\partial w_0}{\partial y} \right) + \left(v_{yy} - v_{yy}^* \right)\delta w_0 \right\}_y dx \Big\rangle dt = 0
\end{aligned} \tag{28}$$

In the above equation, (v_x, v_y), and I_0 (referred to as the inertia) are given by

$$v_{xx} = \frac{\partial M_{xx}}{\partial x} + 2\frac{\partial M_{xy}}{\partial y^2} + N_{xx}\frac{\partial w_0}{\partial x} + N_{xy}\frac{\partial w_0}{\partial y} \tag{29a}$$

$$v_{yy} = \frac{\partial M_{yy}}{\partial y} + 2\frac{\partial M_{xy}}{\partial x^2} + N_{xy}\frac{\partial w_0}{\partial x} + N_{yy}\frac{\partial w_0}{\partial y} \tag{29b}$$

$$I_0 = \int_{-\frac{h}{2}}^{\frac{h}{2}} \rho(z)dz \tag{30}$$

Invoking the arbitrary and independent character of variations $\delta u_0, \delta v_0, \delta w_0, \delta(\partial w_0/\partial x)$, and $\delta(\partial w_0/\partial y)$ one obtains the equations of motion and as a by-product the boundary terms or conditions. This results in three equations of motion in terms of the global stress resultants and stress couples and the four boundary conditions along the plate edges. These equations of motion and boundary conditions can be respectively expressed as

$$\delta u_0: \quad \frac{\partial N_{xx}}{\partial x} + \frac{\partial N_{xy}}{\partial y} = 0 \tag{31a}$$

$$\delta v_0: \quad \frac{\partial N_{yy}}{\partial y} + \frac{\partial N_{xy}}{\partial x} = 0 \tag{31b}$$

$$\begin{aligned}
&\frac{\partial^2 M_{xx}}{\partial x^2} + 2\frac{\partial^2 M_{xy}}{\partial x \partial y} + \frac{\partial^2 M_{yy}}{\partial y^2} + \frac{\partial}{\partial x}\left(N_{xx}\frac{\partial w_0}{\partial x} \right. \\
\delta w_0: \ &\left. + N_{xy}\frac{\partial w_0}{\partial y} \right) + \frac{\partial}{\partial y}\left(N_{yy}\frac{\partial w_0}{\partial y} + N_{xy}\frac{\partial w_0}{\partial x} \right) + P_t \\
&- C\dot{w}_0 = I_0\ddot{w}_0
\end{aligned} \tag{31c}$$

The boundary conditions become

Along the edges $x = 0, L_1$

Either $N_{xx} = N_{xx}^*$ (32a)

or $u_0 = 0$ (32b)

Either $N_{xy} = N_{xy}^*$ (33a)

or $v_0 = 0$ (33b)

Either $M_{xx} = M_{xx}^*$ (34a)

or $$\frac{\partial w_0}{\partial x} = 0 \quad (34b)$$

Either $$V_{xx} = V_{xx}^* \quad (35a)$$

or $$w_0 = 0 \quad (35b)$$

Along the edges $y = 0, L_2$

Either $$N_{yx} = N_{yx}^* \quad (36a)$$

or $$u_0 = 0 \quad (36b)$$

Either $$N_{yy} = N_{yy}^* \quad (37a)$$

or $$v_0 = 0 \quad (37b)$$

Either $$M_{yy} = M_{yy}^* \quad (38a)$$

or $$\frac{\partial w_0}{\partial y} = 0 \quad (38b)$$

Either $$V_{yy} = V_{yy}^* \quad (39a)$$

or $$w_0 = 0 \quad (39b)$$

For the case of all edges simply supported and freely movable the boundary conditions are as follows:

$$\begin{aligned} w_0 = M_{xx} = N_{xy} = 0, N_{xx} = N_{xx}^* \text{ on } x = 0, L_1 \\ w_0 = M_{yy} = N_{yx} = 0, N_{yy} = N_{yy}^* \text{ on } y = 0, L_2 \end{aligned} \quad (40)$$

It should be mentioned for clarification sake that for compressive edge loading $N_{xx}^* = -N_{xx}^0, and\ N_{yy}^* = -N_{yy}^0$.

6. AIR-BLAST LOADING

With the ever increasing demands for increased safety for the solders in the field to operate structurally sound vehicles in the event of an improvised explosive device (IED) or some other type of explosive, it is imperative that an understanding of the structural response of various components within military combat vehicles under an explosive blast be understood so that measures can be taken from a design standpoint to ensure the durability and survivability of these components. To begin to achieve this understanding, the type of explosive loading considered here is a free in-air spherical air burst. Such an explosion creates a spherical shock wave which travels radially outward in all directions with diminishing velocity. The form of the incident blast wave from a spherical charge is shown in figure 4. Where P_{S0} is the peak overpressure above ambient pressure, P_0 is the ambient pressure, t_a is the time of arrival, t_p is the positive phase duration of the blast wave, and t is the time. The waveform shown in figure 4 is

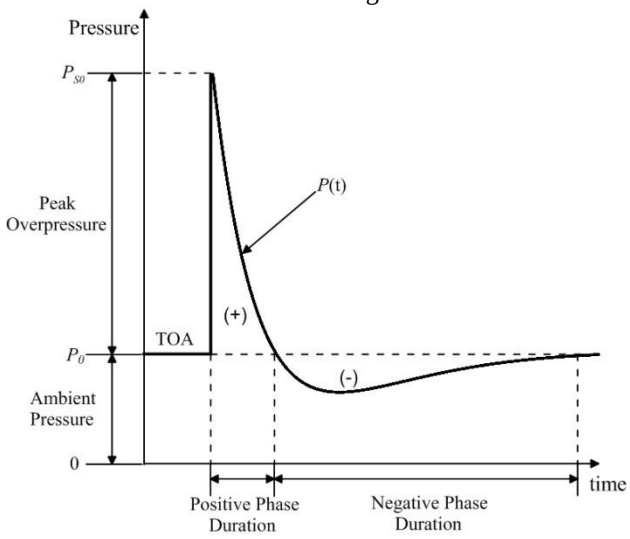

Figure 4: Incident pressure profile of a blast wave.

given by an expression Known as the Friedlander equation and is given as

$$P_t(t) = (P_{S0} - P_0)\left(1 - \frac{t - t_a}{t_p}\right) e^{-\alpha\left(\frac{t-t_a}{t_p}\right)} \quad (41)$$

Where

$$P_{S0} = \frac{1772}{Z^3} - \frac{114}{Z^2} + \frac{108}{Z} \quad (42)$$

In equations (41) and (42) Z is known as the scaled distance given by $Z = R/W^{1/3}$ with R being the standoff distance in meters and W being the equivalent charge weight of TNT in terms of kilograms. Also, α is known as the decay parameter which is determined by adjustment to a pressure curve from a blast test.

For the conditions of standard temperature and pressure (STP) at sea level, the time of arrival t_a, and the positive phase duration t_p, can be determined from [4]

$$\frac{t}{t_1}=\frac{R}{R_1}=\left(\frac{W}{W_1}\right)^{\frac{1}{3}} \tag{43}$$

Where t_1 represents either the arrival time or positive phase duration for a reference explosion of charge weight W_1, and t represents either the arrival time or positive phase duration for any explosion of charge weight W. The determination of the standoff distance for any charge weight W follows a similar reasoning. The application of these relationships is known as cube root scaling. It should be understood that in applying these relationships that the standoff distances are themselves scaled according to the cube root law.

7. SOLUTION METHODOLOGY

To satisfy the first two equations of motion, equations (31a,b), a stress potential will be utilized which allows the in-plane stress resultants to be expressed by letting

$$N_{xx}=\frac{\partial^2\phi}{\partial y^2}, N_y=\frac{\partial^2\phi}{\partial x^2}, N_{xy}-\frac{\partial^2\phi}{\partial x\partial y}. \tag{44}$$

The third equation of motion, equation (31c), can be expressed in terms of two unknown variables, the stress potential ϕ and the transverse displacement w_0. To accomplish this, a partial inversion, of equation (18), the details of which are not presented here, needs to be carried out. Performing a partial inversion results in [4]

$$\begin{Bmatrix}\varepsilon^{(0)}\\ M-M^T\end{Bmatrix}=\begin{bmatrix}[A^*] & [B^*]\\ -[B^*]^T & [D^*]\end{bmatrix}\begin{Bmatrix}N-N^T\\ \varepsilon^{(1)}\end{Bmatrix} \tag{45}$$

Where,

$$\left[A^*\right]=[A]^{-1},\ \left[B^*\right]=-[A]^{-1}[B]\ ,\ -\left[B^*\right]^T=[B][A]^{-1}$$
$$\left[D^*\right]=[D]-[B][A]^{-1}[B] \tag{46}$$

Using Equations (44), (45), and (46) and simplifying, Equation (31c) takes the form

$$D\nabla^4 w_0-\left(\frac{\partial^2\phi}{\partial x^2}\frac{\partial^2 w_0}{\partial y^2}-2\frac{\partial^2\phi}{\partial x\partial y}\frac{\partial^2 w_0}{\partial x\partial y}+\frac{\partial^2\phi}{\partial y^2}\frac{\partial^2 w_0}{\partial x^2}\right)+ \tag{47a}$$
$$I_0\ddot{w}_0+C\dot{w}_0=P_t+\theta\nabla^2N^T+\nabla^2M^T$$

Where,

$$D=\frac{E_1E_3-E_2^2}{E_1(1-\nu^2)},\quad \theta=-\frac{E_2}{E_1} \tag{47b,c}$$

This gives one governing equation with two unknowns, w_o and ϕ. One more equation is needed in terms of the same unknowns which will give two equations in terms of two unknowns which can then be solved. This will come from the compatibility equation. By eliminating the in-plane displacements from the strain-displacement relationships, equations (14) the relationship between the in-plane strains and the transversal deflection known as the compatibility equation can be shown to be given by

$$\frac{\partial^2\varepsilon_{xx}^0}{\partial y^2}+\frac{\partial^2\varepsilon_{yy}^0}{\partial x^2}-\frac{\partial^2\gamma_{xy}^0}{\partial x\partial y}=\left(\frac{\partial^2 w_0}{\partial x\partial y}\right)^2-\frac{\partial^2 w_0}{\partial x^2}\frac{\partial^2 w_0}{\partial^2 y} \tag{48}$$

In view of equations (44) , (45), and (46), the compatibility equation is expressed as

$$\nabla^4\phi=E_1\left[\left(\frac{\partial^2 w_0}{\partial x\partial y}\right)-\frac{\partial^2 w_0}{\partial x^2}\frac{\partial^2 w_0}{\partial^2 y}\right]-(1-\nu)\nabla^2N^T \tag{49}$$

In equations (47) and (49), $\nabla^2=\partial^2/\partial x^2+\partial^2/\partial y^2$ where ∇ is referred to as the Laplacian operator.

Equations (47a) and (49) are the basic governing equations used to investigate the structural response of FG plates under external excitation loading. For the purposes of this paper, from this point forward, the thermal terms will be discarded. To this end, to solve equations (47a) and (49), the approach adopted from [2] will be utilized. In this respect, the following functional forms are assumed for w_o and ϕ [2].

$$w_0(x,y,t)=w_{mn}(t)\sin\lambda_m x\sin\mu_n y \tag{50a,b}$$
$$\phi=A_{mn}(t)\cos 2\lambda_m x+B_{mn}(t)\cos 2\mu_n y+$$
$$C_{mn}(t)\cos 2\lambda_m x\cos 2\mu_n y+D_{mn}(t)\sin 2\lambda_m x\sin 2\mu_n y+$$
$$\frac{1}{2}N_{xx}^*y^2+\frac{1}{2}N_{yy}^*x^2$$

Where $\lambda_m = m\pi/L_1, \mu_n = n\pi/L_2, m,n = 1,2,...$ are the number of half waves in the x and y directions, respectively, and $w_{mn}(t)$ is the amplitude of deflection. Also, $A_{mn}(t), B_{mn}(t), C_{mn}(t),$ and $D_{mn}(t)$ are coefficients to be determined. By substituting equations (50a,b) into equation (49), the coefficients $A_{mn}(t), B_{mn}(t), C_{mn}(t),$ and $D_{mn}(t)$ are determined as

$$A_{mn}(t) = \frac{E_1 w_{mn}^2(t)\mu_n^2}{32\lambda_m^2}, B_{mn}(t) = \frac{E_1 w_{mn}^2(t)\lambda_n^2}{32\mu_m^2}, \quad C_{mn}(t) = D_{mn}(t) = 0 \tag{51}$$

By letting,

$$P_t(t) = P_{mn}(t)\sin\sin\lambda_m x \sin\mu_n y \tag{52a}$$

which implies through integration of both sides over the plate area that

$$P_{mn}(t) = \frac{4}{L_1 L_2}\int_0^{L_2}\int_0^{L_1} P_t(t)\sin\lambda_m x \sin\mu_n y dx dy \tag{52b}$$

or through integration gives

$$P_{mn}(t) = \frac{16P_t(t)}{\pi^2}, \qquad (m,n) = (1,1) \tag{52c}$$

and introduction of equations (50a,b) and (51) into equation (47a) and retaining the resulting equation along with the unsatisfied boundary conditions in the energy functional and applying the Extended Galerkin technique results in the following nonlinear differential equation governing the structural response of FG plates, under external excitation.

$$\ddot{w}_{mn}(t) + 2\Delta_{mn}\omega_{mn}\dot{w}_{mn}(t) + \omega_{mn}^2 w_{mn}(t) + \Omega_{mn}(t)w_{mn}^3(t) = \tilde{P}_{mn}(t) \tag{53}$$

Where, $w_{mn}(t)$ represents the amplitude of deflection of the plate as a function of time, $\tilde{P}_{mn}(t) = 16P_t(t)/I_0\pi^2$, $\omega_{mn} = \sqrt{K_{mn}/I_0}$ is the natural frequency of the FG plate, and $\Delta_{mn} = C/2I_0\omega_{mn}$ is the non-dimensional damping factor, and $\Omega_{mn} = E_1(\lambda_m^4 + \mu_n^4)/16$. It should be noted that at the center of the plate $(x,y) = (L_1/2, L_2/2)$, $w_{mn}(t)$ is equal to the maximum deflection of the plate. In these latter expressions,

$$K_{mn} = \frac{\left(E_1E_3 - E_2^2\right)\pi^4}{\left(1-\nu^2\right)E_1L_1^4}\left(m^4 + 2m^2n^2\psi^2 + n^4\psi^4\right) + \frac{N_{xx}^*\pi^2}{L^2}\left(m^2 + n^2\Phi\psi^2\right) \tag{54}$$

Where,

$\psi = L_1/L_2$ is referred to as the aspect ratio and $\Phi = N_{yy}^*/N_{xx}^*$ is referred to as the compressive/tensile edge load ratio.

Equation (53) is a nonlinear equation in terms of the plate deflections as a function of time. It is interesting to note that equation (53) is very similiar to Duffing's Equation. To obtain the plate deflections as a function of time, equation (53) is solved using the Fourth-Order Runge-Kutta Method.

8. RESULTS AND DISCUSSION

To validate the present theory, comparisons are made with Akay [1] who considered a step loading excitation of a simply supported elastic plate based on a von-karman nonlinear theory. To make this comparison the external excitation, $P_t(t)$, expressed as

$$P_t(t) = P[H(t) - H(t-t_0)]$$

was applied. $H(t)$ is referred to as the Heaviside Step function defined as $H(t) = 1$ for $t \geq 0$ and $H(t) = 0$ for $t < 0$.

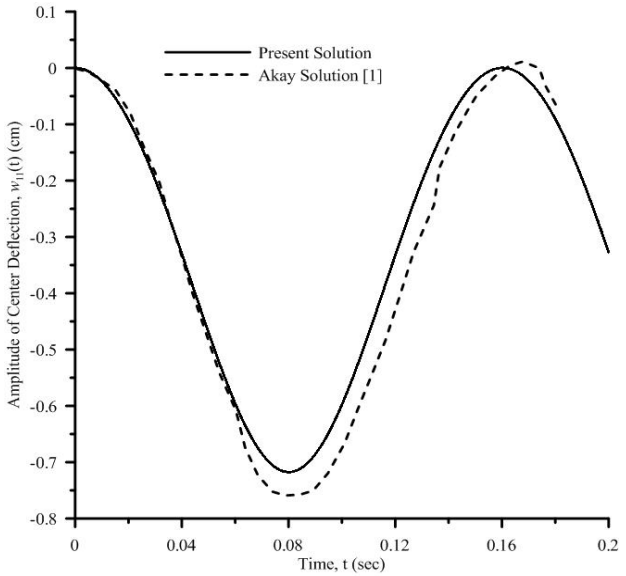

Fig 5. Comparisons of solutions of the time history of the Central deflection Under a Step Load

The geometrical and material properties used were,

$$L_1 = 2.438\,m, \quad h = 0.00635\,m, \quad \psi = 1$$
$$E_m = 70.3\,GPa, \quad \rho_m = 2547\,kg/m^3, \quad \nu_{ave} = 0.25$$

In addition, the constant pressure and time duration were taken as $P = 48.82\,Pa$, $t_0 = 0.2\,\text{sec}$. Since only a metallic isotropic plate was made for comparison, the volume fraction index was taken as $N = 2000$ which implies fully metal. With this in hand, the central deflection time history is displayed in Fig 5. The results in this figure reveal close agreement between Akay's finite element method and the present analytical/ approximation method employed here in the present analysis.

To illustrate the present approach, a ceramic-metal functionally graded plate consisting of Ti-6Al-4V and Aluminum Oxide with the following material properties, which were adopted from [9], were considered for the numerical results presented.

$$E_c = 320.24\,\text{GPa}, \quad \rho_c = 3750\,\text{kg}/m^3, \quad \nu_c = 0.26$$
$$E_m = 105.7\,\text{GPa}, \quad \rho_m = 4429\,\text{kg}/m^3, \quad \nu_m = 0.2981$$
$$\nu_{ave} = 0.2791$$

The geometrical properties used for the FG Plate are $L_1 = 1\,\text{m}$, $\psi = L_1/L_2 = 1$, and unless otherwise stated $h = 0.0254\,\text{m}$ and the halfwaves, (*m*,*n*) = (1,1). In addition, the following reference values, in Table 1. were utilized to determine the time of arrival and positive phase duration [5].

Table 1. Airblast Parameters Versus Distance for a One Kilogram (W_1) TNT Spherical Air Burst [5].

Standoff Distance, R_1 (m)	Arrival Time, t_{a_1} (msec)	Positive Phase Duration, t_{p_1} (msec)
1.0	0.532	1.79

In Fig 6, comparisons of the central deflection of the plate for various volume fraction indexes is depicted. it can be seen that the symmetric functionally graded case with a volume fraction index of *N*=0.5 gives the lowest deflections as a function of time, as compared to the fully metal isotropic case.

Fig 7. Is the counter part of Fig 6. With the exception of the effect of damping. The effect of damping shows a rapid attenuation of the deflections over a very short period of time. It is shown that damping plays a major role in the decrease of deflections of the plate.

In Fig 8. It can be seen that the effects of various amounts of damping on the central deflections vs time attenuates faster as the amount of damping is increased for a fixed volume fraction of the constituent materials. The effects of the compressive/tensile edge loading on a fg plate for a fixed volume fraction index and a fixed amount of damping on the deflection-time response is depicted in Fig. 9. It is clear that, for tensile edge loading, the magnitudes of the deflections decreases in contrast to compressive tensile edge loading where the deflections are increased.

Fig 10. reveals the effects of the aspect ratio on the deflection-time response which indicates that the deflections are larger for smaller aspect ratios than for larger aspect ratios. From a design standpoint, utilizing larger aspect ratio panels would be more beneficial by give smaller deflections under an explosive-type excitation, hence decreased stresses.

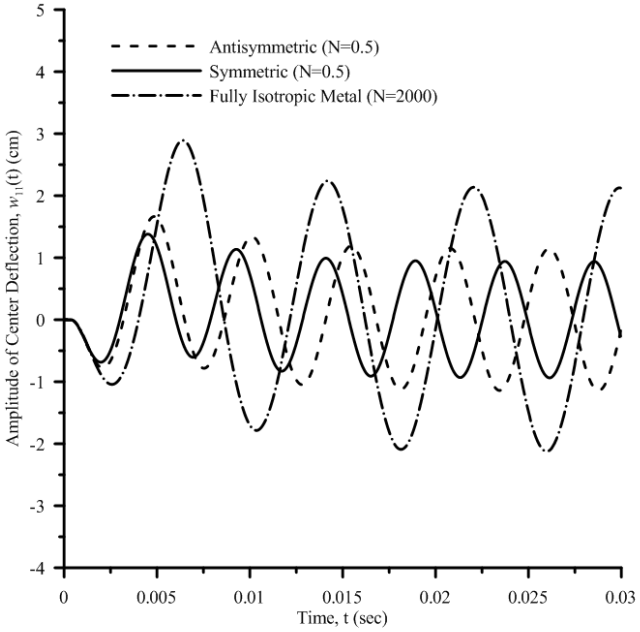

Fig 6. Implications of the volume fraction index on the central deflection as a function of time. (R=0.766 m, t_a=0.000408s, t_p=0.001372s)

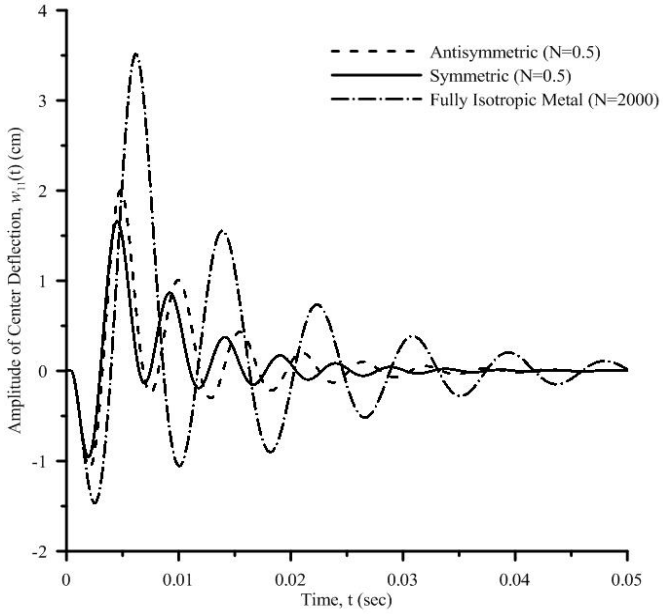

Fig. 7. The counterpart of Fig 6. with a damping measure of Δ_{11}=0.1

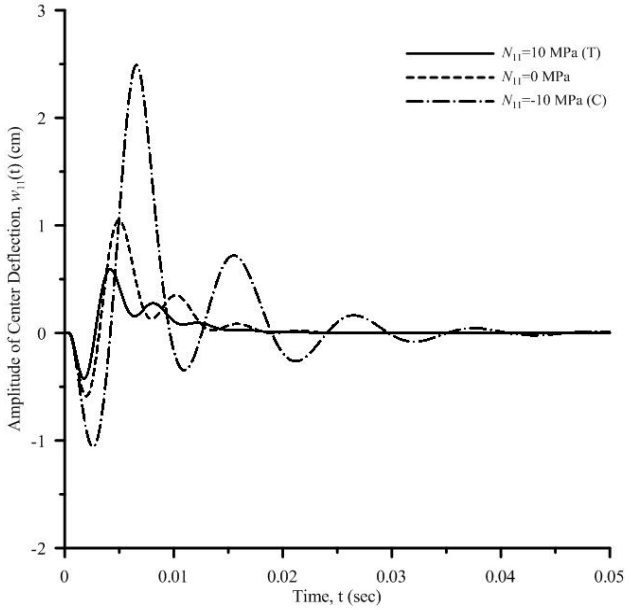

Fig. 9. The implications of the compressive/tensile edge loading on the deflection-time response of an antisymmetric FG plate. (Δ_{11}=0.2, N=0.5)

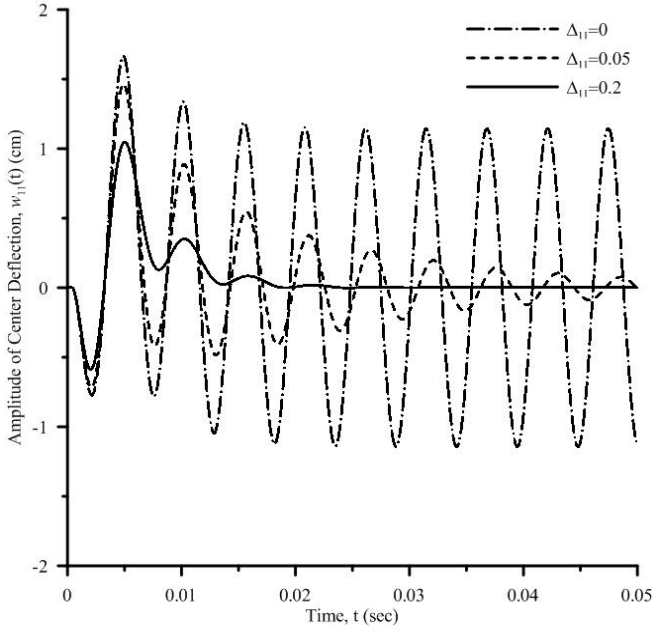

Fig 8. Implications of various amounts of damping on the deflection-time response of an antisymmetric FG Plate. (N=0.5)

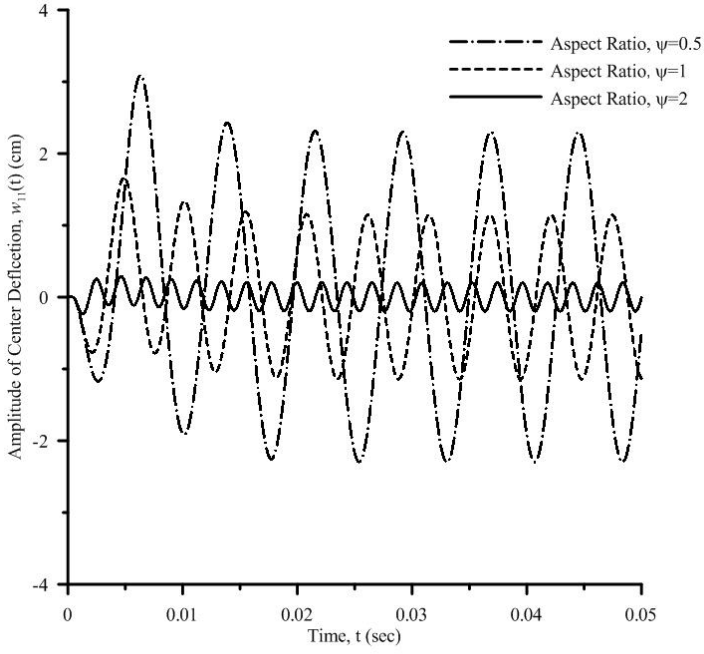

Fig. 10. The effects of various aspect ratios of an antisymmetric FG plate on the deflection-time response. (N=0.5)

9. CONCLUDING REMARKS

A rigorous treatment of functionally graded plates with grading in the transverse direction has been studied. Validations with a simpler transversal excitation step load found in Akay [1], who took a specialized finite element approach, has been made. It has been shown that damping has an important effect when it comes to the attenuation of the deflections. It has also been shown that other factors such as the compressive/ tensile edge loading, the aspect ratio, and the symmetry of the transverse grading throughout the structure plays an important role in the deflection-time history of the structure.

In Fig. 6. It was shown that functionally grading inherently reduces the deflections when compared to the isotropic metallic case. From a design standpoint, it would be appropriate at this point to state that integration of functionally graded materials within plate-type structures would benefit the structural response of the structure. Also, it should be mentioned, although not shown here, that the choice of the ceramic and metal constituent materials chosen would also have a great impact on the response of the structure.

The idea is to reduce the stresses within the structure concerned here. By reducing the magnitude of the deflections, the stresses are reduced. It is hoped and realized that this present study presented here will give insight into some of the factors that can play an important role in the structural response of functionally graded plates and fill in some of the fundamental missing gaps within this subject area.

FUTURE WORK

It should be noted that further work should and needs to be explored which would address comparing finite element blast modeling and simulation results with the current analytical results based on the theory of elasticity. This can be accomplished, by exploring the implementation of these analytical equations, as a user subroutine, in one of the applicable software tools.

ACKNOWLEDGEMENTS

The author would like to express thanks to the U.S. Army-RDECOM-TARDEC for their support and funding under the Independent Laboratory In-house Research program (ILIR).

REFERENCES

[1] Akay, H.U., "Dynamic Large Deflection Analysis of Plates Using Mixed Finite Elements", *Computers and Structures*, Vol. 11, pp. 1-11, Pergamon Press Ltd, 1980.

[2] Hoang Van Tung and Nguyen Dinh Duc, "Nonlinear Analysis of Stability for Functionally Graded Plates Under Mechanical and Thermal Loads", *Composite Structures*, Vol 92, Pgs 1184-1191, 2010.

[3] Hui-Shen Shen, "Functionally Graded Materials-Nonlinear Analysis of Plates and Shells", *CRC Press*, 2009.

[4] Hui-Shen Shen, "Karman-Type Equations for a Higher-Order Shear Deformation Plate Theory and its Use in the Thermal Postbuckling Analysis", *Applied Mathematics and Mechanics*, (English Edition, Vol. 18, No.12, Dec 1997).

[5] Kingery, C.N. and G. Bulmash, "Air-Blast Parameters from TNT Spherical Airburst and Hemispherical Surface Burst", ABRL-TR-02555, U.S. Army Ballistic Research Laboratory, Aberdeen Proving Ground, MD, April 1984.

[6] Reddy, J.N., "Mechanics of Laminated Composite Plates and Shells - Theory and Analysis", 2nd Edition, *CRC Press*, 1997.

[7] Touloukian, Y.S., "Thermophysical properties of high temperature solid materials", MacMillian, N.Y., 1967

[8] Tso-Liang Teng, Cho-Chung Liang, and Ching-Cho Liao, "Transient Dynamic Large-Deflection Analysis of Panel Structure Structure Under Blast Loading", *JSME International Journal*, Series A, Vol. 39, No. 4, 1996.

[9] Xiao-Lin Huang and Hui-Shen Shen, "Nonlinear Vibration and Dynamic Response of Functionally Graded Plates in Thermal Environments", *In ternational Journal of Solids and Structures*, Vol 41, Pgs 2403-2427, 2004.

[10] Young-Wann Kim, "Temperature Dependent Vibration Analysis of Functionally Graded Rectangular Plates", *Journal of Sound and Vibration*, Vol. 248, Pgs 531-549, 2005.